Influence of baseline oscillations on SAR interferometric phase

WANG Bingnan[1,2], ZHANG Fan[1], XIANG Maosheng[1]

1. National Key Laboratory of Microwave Imaging Technology, Institute of Electronics, Chinese Academy of Sciences, Beijing 100190, China;
2. Graduate School of Chinese Academy of Sciences, Beijing 100039, China

Abstract: A model analyzing the effect of baseline oscillations on InSAR phase error is presented in this paper. By a baseline oscillations model, which includes horizontal oscillation and perpendicular oscillation, the models for SAR complex image of slave antenna and interferometric phase error are both deduced. Then effect of baseline oscillations on interferometric phase and quality of SAR image is analyzed. At last, a computer simulation on SRTM system is given. Through raw signal simulation of InSAR in time domain, raw signal for point target and extended scene targets are simulated. After imaging, complex image pairs and interferometric phase are obtained. The simulation results proved the validity of analysis.

Key words: interferometric SAR, interferometric phase, baseline oscillations, raw signal

CLC number: TP722.6 **Document code:** A

Citation format: Wang B N, Zhang F and Xiang M S. 2010. Influence of baseline oscillations on SAR interferometric phase. *Journal of Remote Sensing*. **14**(6): 1171—1181

1 INTRODUCTION

Interferometric synthetic aperture radar (InSAR) has been demonstrated as a topographic mapping technique developed from SAR. It reconstructs digital elevation model (DEM) by relating the signals from two spatially separated antennas over the same scene. InSAR has two work mode-repeat pass mode and single pass mode. In the former mode, temporal decorrelation and decorrelation due to rotation decrease the correlation of image pairs. In single pass mode, two images can be obtained by a single system with two antennas. It wins higher height precision than the former and has a wide application in topographic mapping. In recent world, practical dual-antenna InSAR system has been developed successfully, such as AirSAR and SRTM in America, DOSAR in German.

Stable baseline is the foundation of height precision of InSAR measurement system. However, baseline oscillation is usually unavoidable during radar platform flying. When baseline is long enough, baseline can not be considered as rigid system. Taking SRTM for example, baseline extends to 60 m which belongs to non-rigid structure. Non-rigid baseline structure oscillates during the radar platform flying. Baseline oscillation causes the antenna phase center (APC) deviation, which generates phase errors in raw signal.

Baseline oscillation not only has a bad effect on complex image quality, but also influences the quality of interferogram. This factor has become a vital technology in motion compensation. Little works on raw baseline oscillation has been published in recent years. Franceschetti *et al.* (2000) analyzed effect of mast motion on SRTM performance in frequency domain (Franceschetti *et al*., 1992 & 1998). Mori *et al.* (2004) adopted time domain raw signal simulator to analyze motion errors' influence on the image and phase error qualitatively. However, they did not develop the interferometric phase error model quantitatively, but focus on qualitative analysis. They also have not deceived the equation of interferometric phase error caused by baseline oscillation.

Based on a baseline oscillations model, this paper proposed complex image model of slave antenna and interferometric phase error model due to baseline oscillation. Influence of baseline oscillation on SAR image quality and interferometric phase is analyzed in detail. Raw signal for point target and extended scene targets are simulated to prove the theoretical analysis. Interferometric phase error model helps us study the influence of non-rigid baseline oscillation on interferometric phase. It plays a great role in SAR imaging and motion compensation.

2 BASELINE OSCILLATION MODEL

For non-rigid baseline radar system (SRTM, GeoSAR), its stretching, roll and yaw effects on SAR raw signal can not be neglected. In Fig.1, reference frame *XYZ* originates in the main antenna phase center and *X* is along the direction of platform velocity, and *Y* is along the ground range direction. S_1S_2 are main antenna and slave antenna phase center respectively. Baseline oscillation can be divided into two parts: horizontal

Received: 2009-12-10; **Accepted**: 2010-05-19

Foundation: The national basic research program of china (No. 2009CB724003).

First author biography: WANG Bingnan (1984—), male. Ph.D candidate in signal and information management in the Institute of Electronics, Chinese Academy of Sciences. He majors in InSAR simulation and processing. E-mail: wangbingnan05@gmail.com

oscillation and perpendicular oscillation. The oscillation angles are defined in Fig.1. $S_1S'_2$ is the projection of S_1S_2 in S_1YZ plane. $S_1S''_2$ is the projection of S_1S_2 in S_1YZ plane without baseline oscillation. Then perpendicular oscillation angle α_r can be defined as the angle between $S_1S'_2$ and $S_1S''_2$ and horizontal oscillation angle α_a is the angle between baseline vector S_1S_2 and S_1YZ plane. Usually, baseline does not oscillate in single frequency, but any form of function can be divided into summation of sinusoidal with different frequency. oscillation angle can be demonstrated as shown in Eq.(1):

$$\alpha_{a,r} = \sum A_{a,r} \sin(2\pi f_{ba,br}(t - t_0) + \phi_{a,r}) \tag{1}$$

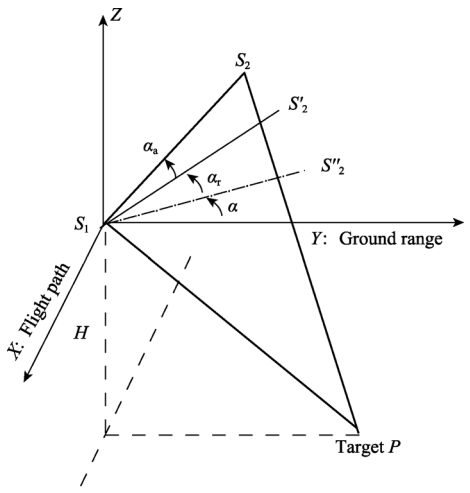

Fig. 1 Slave antenna oscillation model

where $A_{a,r}$ is the amplitude of oscillation, $f_{ba,br}$ is the oscillation frequency, and $\phi_{a,r}$ is the initial phase. In order to introduce baseline oscillation, slant range between radar and target should be calculated. Assume that APC of main antenna has no deviation, slave antenna oscillates. In Fig.1, coordinates of target P in reference frame S_1-XYZ are (x_p,y_p,z_p). Coordinates of main antenna APC is (x_{s1},y_{s1},z_{s1}), where y_{s1} and z_{s1} is equal to zero. Without oscillation, coordinates of slave antenna APC are $(x_{s1}, y_{s1} + B\cos\alpha, z_{s1} + B\sin\alpha)$, where B is length of baseline, and α is tilt angle of baseline. When baseline oscillation occurs, horizontal and perpendicular oscillation angles are α_a and α_r respectively. Then coordinates of slave antenna $(x'_{s2}, y'_{s2}, z'_{s2})$ can be computed as follows.

$$\begin{aligned} x'_{s2} &= x_{s1} + B\sin\alpha_a \\ y'_{s2} &= y_{s1} + B\cos\alpha_a\cos(\alpha + \alpha_r) \\ z'_{s2} &= z_{s1} + B\cos\alpha_a\sin(\alpha + \alpha_r) \end{aligned} \tag{2}$$

In Eq.(2), horizontal oscillation angle α_a is almost equal to zero, so $\cos\alpha_a \approx 1$. Then coordinates of slave antenna in reference frame can be simplified as: $(x_{s1} + B\sin\alpha_a, y_{s1} + B\cos(\alpha + \alpha_r), z_{s1} + B\sin(\alpha + \alpha_r))$. It can be seen that horizontal oscillation causes coordinate of slave antenna in X direction deviate and perpendicular oscillation affects its coordinates in both Y and Z direction. Eq.(3) shows the range between slave antenna APC and target P. Slant range not only affects SAR image quality but also influences its phase. For InSAR system, baseline oscillations bring interferometric phase error, and decrease quality of interferogram. It becomes an unavoidable problem which should be analyzed and resolved.

$$\begin{aligned} R_2 &= \sqrt{(x'_{s2} - x_p)^2 + (y'_{s2} - y_p)^2 + (z'_{s2} - z_p)^2} = \\ &\sqrt{(x_{s1} + B\sin\alpha_a - x_p)^2 + (y_{s1} + B\cos(\alpha + \alpha_r) - y_p)^2 + (z_{s1} + B\sin(\alpha + \alpha_r) - z_p)^2} \end{aligned} \tag{3}$$

3 BASELINE OSCILLATION EFFECT ON INTERFEROMETRIC PHASE

3.1 Baseline oscillation effect on azimuth Doppler frequency modulation (FM) rate

SAR sensor radiates linear frequency modulation signal with frequency modulation rate K and pulse duration T_r. Through coherent receiving, the single point echo is expressed as two-dimensional $s_r(t,\tau)$ (Bao Z *et al*., 2005):

$$\begin{aligned} s_r(t,\tau) &= \sigma w_a^2(t)\exp\left\{-j\frac{4\pi}{\lambda}R(t)\right\}\times \\ &\exp\left\{j\pi K(\tau - \frac{2R(t)}{c})^2\right\}\mathrm{rect}\left\{\frac{\tau - 2R(t)/c}{T_r}\right\} \end{aligned} \tag{4}$$

where t is the azimuth slow time, τ is the range fast time, $w_a(\theta)$ is the azimuth illumination diagram, σ is back scattering coefficient, and rect[] is a rectangular envelope. Considering baseline oscillations, calculate the slant range of slave antenna according to Eq.(3). It can be seen from Eq.(4) that baseline oscillations cause motion error in range but does not influence range FM rate K_r. So it does not affect range compression of SAR raw signal. Therefore, we can make a conclusion that baseline oscillations have no effect on SAR image quality in range direction. This section focuses on the effect of baseline oscillation on azimuth Doppler FM rate.

Assuming that the radar beam is perpendicular to flight path, the distance from target P to flight path can be expressed as: $R_B = \sqrt{{y_p}^2 + {z_p}^2}$. Let the angle between the vector connecting target P to azimuth coordinate and vector perpendicular to flight path is β, then $y_p = R_B\sin\beta$, $z_p = R_B\cos\beta$, so Eq. (3) can be re-written as follows.

$$R_2 = \sqrt{(x_{s1} - x_p + B\sin\alpha_a)^2 + (B\cos(\alpha + \alpha_r) - R_B\sin\beta)^2 + (B\sin(\alpha + \alpha_r) - R_B\cos\beta)^2} \approx R_B + \frac{(vt + \Delta x(t))^2}{2R_B} + \Delta R_r(t) \tag{5}$$

where x_{s1}–x_p is equal to vt, v is equivalent velocity of radar platform, Δx, which is equal to $B\sin\alpha_{\mathrm{a}}(t)$, is azimuth motion error caused by horizontal oscillation, and ΔR_{r}, which is equal to $B\sin\beta\cos(\alpha+\alpha_{\mathrm{r}}(t))+B\cos\beta\sin(\alpha+\alpha_{\mathrm{r}}(t))$, is range error due to baseline oscillation.

Dopller phase of raw signal in azimuth can be described as $-4\pi R_2/\lambda$, then we make the first derivative of Eq.(5) on azimuth slow time. We can get FM rate of azimuth signal in Eq. (6):

$$K_a=\frac{1}{2\pi}\frac{4\pi}{\lambda}\frac{\mathrm{d}^2R_2}{\mathrm{d}t^2}=\frac{2}{\lambda}\frac{\mathrm{d}^2R_2}{\mathrm{d}t^2}=\frac{2v^2}{\lambda R_B}+\frac{2(v\Delta x'+\Delta x'')}{\lambda R_B}+\frac{2\Delta R_{\mathrm{r}}''}{\lambda} \tag{6}$$

where $\Delta x'$ and $\Delta x''$ are the first derivative and the second derivative of $\Delta x'$ on azimuth slow time respectively. $\Delta R_{\mathrm{r}}''$ is the second derivative of ΔR_{r} on azimuth slow time. In Eq. (6), the first item is FM rate in azimuth without baseline oscillation, and the second item is the FM rate error caused by horizontal oscillation. The second item, which changes along range, can be neglected because there is 'R_{B}' in its denominator. So, horizontal oscillation has little effect on image quality. In Eq. (6), the third item is connected to perpendicular oscillation of baseline, which can not be neglected. This item changes the FM rate in azimuth and affects the azimuth compression of SAR raw signal.

3.2 Effect of baseline oscillation on interferometric phase

Section 3.1 has analyzed the effect of baseline oscillation on the image quality from the view of FM rate of raw signal. Based on the signal model of complex image of slave antenna, in this section we focus on the interferometric phase error model caused by baseline oscillation. After range compression, raw signal in Doppler domain can be re-written as Eq.(7) using principle of stationary phase (POSP).

$$s_{\mathrm{r}}(f_{\mathrm{a}},\tau)=Aw_{\mathrm{a}}^2(f_{\mathrm{a}})\sin\mathrm{c}\left[KT_{\mathrm{r}}(\tau-\frac{2R_{\mathrm{rd}}(f_{\mathrm{a}})}{\mathrm{c}})\right]\exp\left\{-\mathrm{j}\frac{4\pi}{\lambda}R_{\mathrm{rd}}(f_{\mathrm{a}})\right\} \tag{7}$$

where $R_{\mathrm{rd}}(f_{\mathrm{a}})$ is the range cell migration in doppler domain, $R_{\mathrm{rd}}(f_{\mathrm{a}})=R_2(t_{\mathrm{s}})$, t_{s} is the point of stationary phase. After the precise range cell migration correction, azimuth compression can be finished in frequency domain by matched filtering, and then processed signal can be rewritten in Eq. (8):

$$s_1(f_{\mathrm{a}},\tau)=Aw_{\mathrm{a}}^2(f_{\mathrm{a}})\sin\mathrm{c}\left[KT_{\mathrm{r}}(\tau-\frac{2R_B}{\mathrm{c}})\right]\exp\left\{-\mathrm{j}\frac{4\pi}{\lambda}R_B\right\}\times\exp\left\{-\mathrm{j}\frac{4\pi}{\lambda}(\frac{\Delta x^2(t_{\mathrm{s}})+2vt_{\mathrm{s}}\Delta x(t_{\mathrm{s}})}{2R_B}+\Delta R_{\mathrm{r}}(t_s))\right\} \tag{8}$$

Eq. (8) expresses the range Doppler spectrum of complex SAR image. The last exponential item is phase error of image because of baseline oscillation. This item will generate additional phase error and it brings new error to interferometric phase. Make an inverse FFT on Eq. (8).

$$s_2(t,\tau)=A\sin\mathrm{c}\left[KT_{\mathrm{r}}(\tau-\frac{2R_B}{\mathrm{c}})\right]\exp\left\{-\mathrm{j}\frac{4\pi}{\lambda}R_B\right\}\times\int_{-B_{\mathrm{d}}/2}^{B_{\mathrm{d}}/2}w_{\mathrm{a}}^2(f_{\mathrm{a}})\exp\left\{-\mathrm{j}\frac{4\pi}{\lambda}\Delta\phi(f_{\mathrm{a}})\right\}\exp(\mathrm{j}2\pi f_{\mathrm{a}}t)\mathrm{d}f_{\mathrm{a}} \tag{9}$$

where $\Delta\phi(f_{\mathrm{a}})=\frac{\Delta x^2(t_{\mathrm{s}})+2vt_{\mathrm{s}}\Delta x(t_{\mathrm{s}})}{2R_B}+\Delta R_{\mathrm{r}}(t_{\mathrm{s}})$ is the phase error caused by baseline oscillation. When the baseline oscillation does not exist, this item is equal to zero. Then the result of integral has the form of 'sinc' function, which is coherent to the ideal expression. When this integral item exists, it affects azimuth focus of raw signal. This conclusion is coherent to analysis in section 3.1. Further more, integral item brings additional phase error, which is the error caused by baseline oscillation. In azimuth, $\frac{\Delta x^2(t_{\mathrm{s}})+2v.t_{\mathrm{s}}.\Delta x(t_{\mathrm{s}})}{2R_B}<<\Delta R_{\mathrm{r}}(t_{\mathrm{s}})$ is negligible, then integral item can be calculated using POSP:

$$\exp\left\{\mathrm{j}(-\frac{4\pi}{\lambda}\Delta\phi(f_{\mathrm{as}})+2\pi f_{\mathrm{as}}t)\right\}=\exp\left\{\mathrm{j}(-\frac{4\pi}{\lambda}A_{\mathrm{r}}B\cos\beta\cos(\frac{2\pi f_{\mathrm{br}}}{K_{\mathrm{a}}}f_{\mathrm{as}})+2\pi f_{\mathrm{as}}t)\right\} \tag{10}$$

where f_{as} is stationary phase point. Eq.(10) is what we want to deduce the interferometric phase model. It is composed of cosine function and linear function. When stationary phase point $2\pi(f_{\mathrm{br}}/K_{\mathrm{a}})f_{\mathrm{as}}$ is close to zero, connection between stationary phase point f_{as} and slow time t satisfy linear exp- ression. According to Eq. (10), we can make some conclusions as following: (1) Interferometric phase error is close to sinusoidal. (2) Interferometric phase error frequency is in pro- portion to frequency of baseline oscillation. The faster baseline oscillates, the quicker interferometric phase error becomes. (3) Amplitude of Interferometric phase error is in proportion to amplitude of baseline oscillation. The larger baseline oscillation amplitude is, the bigger amplitude of interferometric phase error becomes, and interferogram becomes worse.

4 SIMULATION EXAMPLE

In order to verify analytical result above, we give some simulation examplein in this section. Firstly, Interferometric SAR raw signal is simulated. By imaging and processing, interferogram can be obtained. Simulation parameters adopt space shuttle in SRTM, which is shown in Table 1 and Table 2. Raw signal simulation model includes geometric model, backscattering coefficient model and raw signal model. Geometric model takes earth rotation, ellipsoid and non-line orbit into consideration. Being calculated in inertia reference frame, the computation becomes very complicated. We adopt the method of coordinate transformation here to simplify this problem (Wei, 2001). Backscattering coefficient model are extracted by Ulaby and Dobson for a given terrain, frequency band and polarization

(Ulaby & Dobson, 1988) shown in Eq. (11).

$$\sigma^0(\mathrm{dB}) = P_1 + P_2 \exp(-P_3\theta) + P_4 \cos(P_5\theta + P_6) \quad (11)$$

Table 1 SRTM orbit parameters

Orbit parameters	Value
Period/s	5349.0412
Perigee altitude/km	220
Apogee altitude/km	245
Orbit altitude/km	233
Orbit inclination/(°)	57

Table 2 SAR parameters

Radar Parameters	Value
Wave length/m	0.03125
Pulse bandwidth/MHz	9.5
Pulse duration/μs	40
PRF/Hz	1488
Sampling rate/MHz	11.4
Look angle/(°)	45
Main antenna dimension/m^2	12×0.4
Slave antenna dimension/m^2	12×0.4
Baseline lenth/m	60

where θ is incident angle, P_{1-6} is decided by signal frequency and classification of scenes, which can be obtained in handbook written by Ulaby and Dobson. We use time domain algorithm-range time domain pulse coherence to simulate raw data (Liu, 1999). In order to illuminate the effect of baseline oscillation on image quality, point target simulation is done and image quality parameters are compared. Then we generate raw data for an extended scene targets and raw data were properly processed.

4.1 Point target simulation

We give a point target simulation to illustrate effect of oscillation on image quality in this section. Baseline horizontal and perpendicular oscillation amplitude and frequency are equal to 0.025° and 2 Hz respectively. Raw signal of point target is obtained and processed. Impulse response function (IRF) in azimuth and range are shown in Fig.2. In Fig.2(a), range IRF are almost identical whether or not baseline oscillation is considered. It proves that baseline oscillation has little effect on range compression. In Fig.2 (b), IRF becomes extended in the case of no baseline oscillation. Furthermore, azimuth resolution goes down, side lobe ratio (SLR) of IRF increases. Amplitude and frequency of oscillation increases, quality of azimuth image decreases.

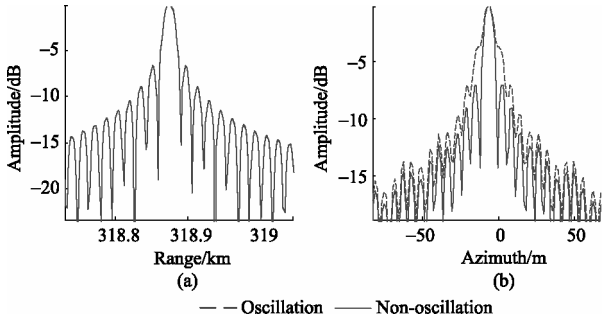

Fig. 2 Impulse response function
(a) Range (Solid and dotted lines are almost identical); (b) Azimuth

Fig.3 describes the effect of baseline horizontal oscillation on image quality, with oscillation amplitude 0.025° and frequency 4 Hz. Assume that there is no perpendicular oscillation. We can see from the Fig.3 that baseline horizontal oscillation has little effect on image quality. This conclusion accords with analysis in section 2. Fig.4 illustrates the error of complex image azimuth spectrum. Continuous line is theore- tical value deduced in section 3, and dotted line is obtained by raw signal simulation. It proves analysis in section 3.

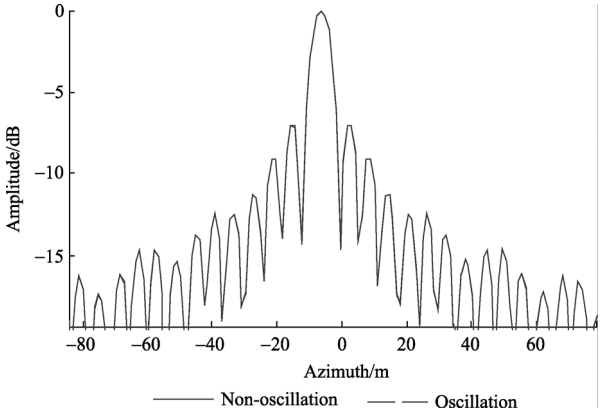

Fig. 3 Horizontal oscillation's effect on imaging (Solid and dotted lines are almost identical)

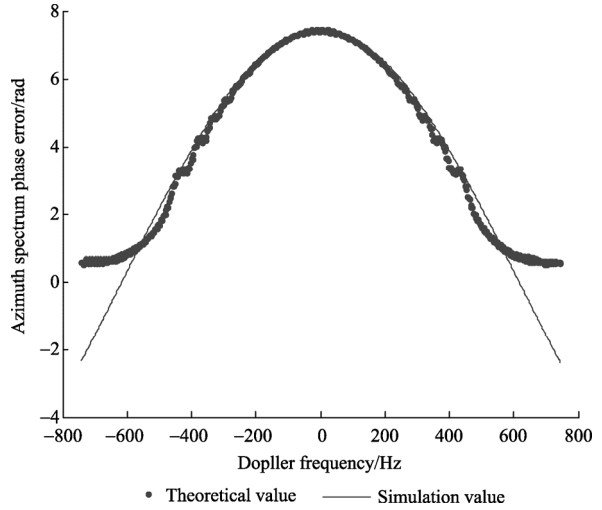

Fig. 4 Azimuth spectrum of complex image

4.2 Extended scene simulation

We focus on the effect of baseline oscillation on interferogram in this section. The extended scene contains 512(azimuth) × 2196(range) scattering points, and digital elevation model (DEM) uses a cone, whose peak height is 500 m. In Fig.5 after raw signal generation and raw data imaging,

there are four explication examples with different amplitude and frequency of baseline oscillation. The length of baseline decreases to 4 m to show interferogram better. We can see from the figure that interferogram becomes blurring and twisting because of oscillation. Fig.5(a) describes interferogram of non baseline oscillation. Make a comparison to Fig.5(b) and Fig.5(c). The amplitude of oscillations in Fig.5(b) and Fig.5(c) are the same. When the oscillation frequency increases, interferogram twists faster. Comparing Fig.5(c) with Fig.5(d), when oscillation frequency is equal, the larger oscillation amplitude is, the bigger interferometric phase error becomes. In Fig.5 (d) periodical blurring exist in azimuth, which make it clear that interferometric phase error changes periodically. All these conclusions are consistent to theoretical analysis.

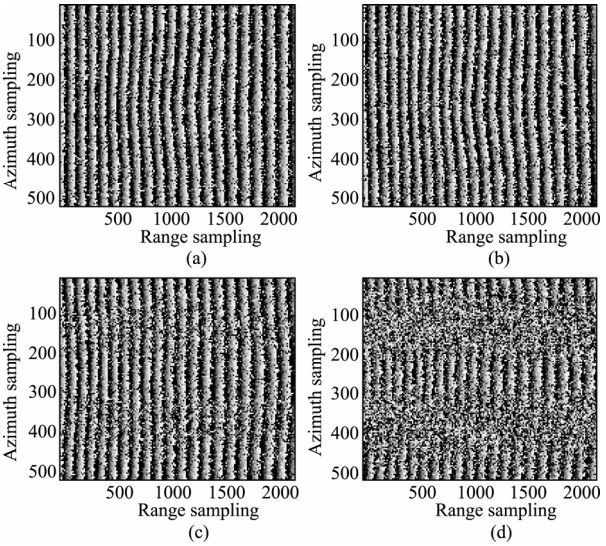

Fig. 5 Effect of baseline oscillation on interferogram
(a) A=0, f=0; (b) A=0.05°, f=1Hz; (c) A=0.05°, f=3Hz; (d) A=0.1° , f=3Hz

Fig.6 gives interferometric phase error caused by different amplitude and frequency of baseline oscillation. The length of baseline is reconfigured as 60 m. When oscillation amplitudes are both 0.05 °C and frequency are 2 Hz and 4Hz respectively, interferometric phase error are close to sinusoidal. Furthermore period of the former is twice of the latter. It can be seen that period of interferometric phase error is equal to oscillation period. When oscillation frequency is both 2 Hz and amplitudes are 0.05° and 0.1° respectively, period of interferometric phase error is equal but amplitude of phase error are not the same. The bigger the amplitude of oscillation, the larger the interferometric phase error becomes.

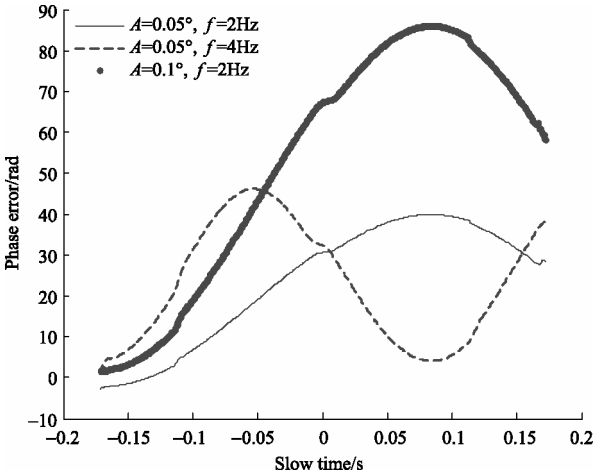

Fig. 6 Interferometric phase error

5 CONCLUSION

In this paper, complex image model and interferometric phase error model are constructed when interferometric baseline oscillates. Effect of horizontal and perpendicular oscillation on image and interferometry are analyzed in detail. Trough raw signal simulation, including point target and extended scene, the validity of theoretical analysis is proved.

REFERENCES

Bao Z, Xing M D and Wang T. 2005. Synthetic Aperture Radar Imaging. Beijing: Publishing House of Electronic Industry

Franceschetti G, Migliaccio M, Riccio D and Schirinzi G. 1992. SARAS: A synthetic aperture radar(SAR) raw signal simulator. *IEEE Trans. on Geoscience and Remote Sensing*, **30**(1): 110—123

Franceschetti G, Iodice A, Migliaccio M and Riccio D. 1998. A novel across-track SAR interferometry simulator. *IEEE Transactions on Geoscience and Remote Sensing*, **36**(3): 952—962

Franceschetti G, Iodice A, Maddaluno S and Ricco D. 2000. Effect of antenna mast motion on X-SAR/SRTM performance. *IEEE Trans. Geosci. Remote Sensing*, **38**(5): 2361—2372

Liu Y T.1999. Radar Imaging Technology. Haerbin: Harbin Institute of Technology Press

Mori A and Vita F D. 2004. A time-domain raw signal simulator for interferometric SAR. *IEEE Transactions on Geoscience and Remote Sensing*, **42**(9): 1811—1817

Ulaby F T and Dobson M C. 1988. Handbook of Radar Scattering Statistics for Terrain. Aretech House Editor

Wei Z Q. 2001. Synthetic Aperture Radar Satellite. Beijing: Science Press

基线抖动对干涉 SAR 相位的影响

汪丙南[1,2], 张 帆[1], 向茂生[1]

1.中国科学院 电子学研究所, 微波成像技术国家级重点实验室, 北京 100190;
2.中国科学院 研究生院, 北京 100039

摘 要: 提出并分析了基线抖动造成的干涉 SAR 相位误差模型。基于干涉 SAR 基线抖动模型, 分为水平抖动和垂直抖动, 推导了存在基线抖动情况下辅天线复图像信号模型及基线抖动带来的干涉相位误差公式, 分析了基线抖动对成像质量和干涉相位的影响, 针对 SRTM 系统进行了计算机仿真。通过基于基线抖动的干涉 SAR 原始回波数据计算, 仿真了点目标和面目标场景的回波信号, 并进行成像得到了复图像和干涉条纹, 仿真结果验证了理论分析的正确性。

关键词: 干涉 SAR, 干涉相位, 基线抖动, 回波

中图分类号: TP722.6 文献标志码: A

引用格式: 汪丙南, 张 帆, 向茂生. 2010. 基线抖动对干涉 SAR 相位的影响. 遥感学报, **14**(6): 1171—1181
Wang B N, Zhang F and Xiang M S. 2010. Influence of baseline oscillations on SAR interferometric phase. *Journal of Remote Sensing*. **14**(6): 1171—1181

1 引 言

干涉 SAR 是在 SAR 基础上发展起来的一种干涉测量技术, 它通过对多个接收天线观测得到的回波数据进行干涉处理, 获得地面高程图(DEM)。干涉 SAR 有两种工作模式: 重复轨道干涉和双天线干涉。由于重复轨道模式带来了时间去相关和多普勒谱偏移去相关, 使得干涉复图像相关性大大减小, 从而降低了干涉图的质量。双天线单航过干涉 SAR 系统具有更高的高程测量精度, 在地形测绘等中得到广泛的应用, 当前研究机构已经成功研制了双天线干涉 SAR 系统, 如美国的 AirSAR, SRTM, 德国的 DOSAR 等。

构建稳定的基线是保证双天线干涉SAR系统高程测量精度的关键, 然而在干涉 SAR 系统工作期间的基线抖动难以避免的。当双天线基线长度足够长时, 基线支撑臂不能看成刚性的系统。以 SRTM 为例, 基线支撑臂长度达到 60m, 属于非刚性结构。非刚性基线结构在运动过程中会产生抖动现象。天线桅杆的抖动造成天线相位中心偏离, 给干涉 SAR 回波信号带来运动误差, 不仅影响成像质量, 更重要的是带来干涉相位误差, 降低干涉图质量, 影响干涉测量精度。

基线抖动不仅给干涉 SAR 成像质量产生影响, 而且影响复图像相位, 带来干涉相位误差。基线抖动成为干涉 SAR 技术中必须解决的关键技术, 运动误差补偿中必须解决的误差因素。国际上开展这方面的研究较少, Franceschetti 等(2000)是基于 SARAS 频域回波仿真器 (Franceschetti 等, 1992 和 1998), 在二维频域内分析基线抖动对 SRTM 系统性能的影响, Mori(2004)采用时域的干涉 SAR 回波信号仿真方法, 仿真并定性地分析了基线抖动对成像质量和干涉相位误差的影响, 没有从机理上推导基线抖动带来的干涉相位误差模型。前人的研究成果主要围绕着定性地分析基线抖动对干涉相位影响, 并没有给出基线抖动带来的干涉相位误差表达式。

本文从建立基线抖动误差模型出发, 提出了存在基线抖动情况下辅天线复图像信号模型和基线抖动造成的干涉相位误差模型, 分析了基线抖动对成像质量和干涉相位带来的影响, 分别对点目标和面

收稿日期: 2009-12-10; 修订日期: 2010-05-19
基金项目: 国家重点基础研究发展计划(973)(编号: 2009CB724003)。
第一作者简介: 汪丙南(1984—), 男, 中国科学院电子学研究所信号与信息处理专业博士研究生, 目前主要从事干涉合成孔径雷达信号仿真和处理研究。E-mail: wangbingnan05@gmail.com。

目标场景回波信号进行了仿真，验证了理论分析的结果。基线抖动干涉相位误差模型的建立，使得我们可以定量的分析柔性基线抖动对回波信号产生的相位的影响，对于干涉 SAR 成像和运动误差补偿有着重要的意义。

2 基线抖动误差模型

对于基线结构非刚性的系统(如SRTM、GeoSAR系统)，基线抖动主要由非刚性基线机械结构的弯曲、扭曲和伸展造成，如图 1，坐标系 XYZ 原点位于主天线相位中心，X 方向是雷达平台速度方向，Y 是地距方向，Z 轴与 XY 构成右手系，S_1 和 S_2 分别是主辅天线相位中心的位置。将基线的抖动分解为水平抖动和垂直抖动。通过图 1 来说明水平抖动角和垂直抖动角的含义。图 1 中 S_1S_2 是实际基线位置，$S_1S'_2$ 是基线在 S_1YZ 平面的投影，$S_1S''_2$ 则是不存在基线抖动的情况下基线的位置。那么水平抖动角 α_a 的含义就是基线与 YS_1Z 平面的夹角，这导致基线在 X 轴方向产生分量。垂直抖动角 α_r 含义为基线在 YS_1Z 平面上投影与基线理想位置($S_1S''_2$)的偏角。在实际情形中，基线水平和垂直抖动并不是单频抖动，但是任何形式的函数可以表示成正弦函数和的形式，因此将水平和垂直抖动角进行谐波分解，如式(1)所示:

$$\alpha_{a,r}=\sum A_{a,r}\sin(2\pi f_{ba,br}(t-t_0)+\phi_{a,r}) \tag{1}$$

式中，$A_{a,r}$ 是抖动幅度，单位为 rad; $f_{ba,br}$ 分别是基线水平和垂直抖动频率；$\phi_{a,r}$ 是 t_0 时刻的的初始相位。为了引入基线臂抖动对 SAR 回波信号的影响，需要建立瞬时斜距模型。先假设主天线不动，辅天线相对主天线发生理想轨迹偏移。如图 1，设目标 P 在 S_1-XYZ 坐标系中的坐标为(x_p,y_p,z_p)，雷达平台主天线相位中心坐标为(x_{s1},y_{s1},z_{s1})，其中 y_{s1}=0，z_{s1}=0。在理想运动状况下，辅天线相位中心坐标(x_{s2},y_{s2},z_{s2})为

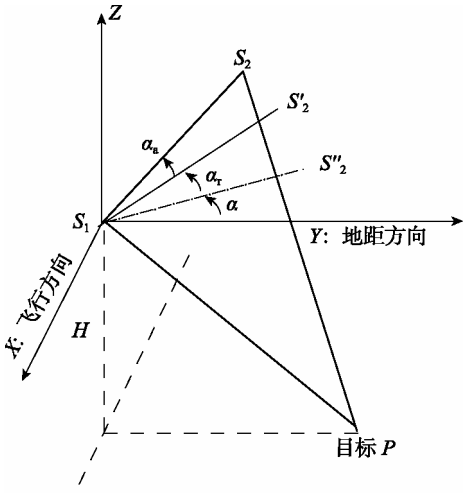

图 1 辅天线抖动模型

$(x_{s1}, y_{s1}+B\cos\alpha, z_{s1}+B\sin\alpha)$，其中 B 是基线长度，α 为基线倾角；当天线桅杆发生抖动，基线水平、垂直抖动角分别为 α_a、α_r。那么辅天线相位中心发生偏离，添加基线抖动影响后辅天线相位中心在坐标系 S_1-XYZ 中的坐标 $(x'_{s2}, y'_{s2}, z'_{s2})$ 表示为:

$$\begin{aligned} x'_{s2}&=x_{s1}+B\sin\alpha_a \\ y'_{s2}&=y_{s1}+B\cos\alpha_a\cos(\alpha+\alpha_r) \\ z'_{s2}&=z_{s1}+B\cos\alpha_a\sin(\alpha+\alpha_r) \end{aligned} \tag{2}$$

式(2)中由于水平基线抖动角 α_a 很小接近 0，因此 $\cos\alpha_a\approx1$，从而辅天线坐标可以进一步简化为 $(x_{s1}+B\sin\alpha_a, y_{s1}+B\cos(\alpha+\alpha_r), z_{s1}+B\sin(\alpha+\alpha_r))$。从辅天线坐标可以看出，天线桅杆水平抖动，造成辅天线相位中心方位向坐标(X轴)发生偏移，而基线垂直抖动造成 Y 轴和 Z 轴坐标发生变化。结合公式辅天线相位中心坐标和目标 P 点坐标，可以计算辅天线瞬时斜距，如式(3)。斜距不仅影响 SAR 成像质量，而且直接影响复图像相位。对于干涉 SAR，基线抖动运动误差直接带来新的干涉相位误差，造成干涉条纹质量下降，对于后续的干涉处理必须分析和解决这一问题。

$$\begin{aligned} R_2&=\sqrt{(x'_{s2}-x_p)^2+(y'_{s2}-y_p)^2+(z'_{s2}-z_p)^2}= \\ &\sqrt{(x_{s1}+B\sin\alpha_a-x_p)^2+(y_{s1}+B\cos(\alpha+\alpha_r)-y_p)^2+(z_{s1}+B\sin(\alpha+\alpha_r)-z_p)^2} \end{aligned} \tag{3}$$

3 基线抖动对干涉相位的影响

3.1 基线抖动对方位多普勒调频率的影响

SAR 发射调频率为 K，脉宽为 T_r 的线性调频信号。经过相干解调后，单点目标的回波信号二维表示为 (保铮等, 2005):

$$\begin{aligned} s_r(t,\tau)&=\sigma w_a^2(t)\exp\left\{-j\frac{4\pi}{\lambda}R(t)\right\}\times \\ &\exp\left\{j\pi K(\tau-\frac{2R(t)}{c})^2\right\}\mathrm{rect}\left\{\frac{\tau-2R(t)/c}{T_r}\right\} \end{aligned} \tag{4}$$

t 是方位向慢时间，τ是距离快时间，$w_a^2(\theta)$ 是双程天线方向图调制，σ是点目标后向散射系数。rect[]是矩形包络。添加基线水平和垂直抖动，辅天线瞬时斜距计算如式(3)。从式(4)回波信号看出，基线抖动造成的瞬时斜距偏离，并没有改变距离信号的调频率 K_r，不会对距离向信号压缩产生影响，因此，基线抖动带来的运动误差对回波信号在距离向成像质量没有产生影响。

在方位处理之前，首先对辅天线瞬时斜距(式(3))进行抛物线近似，设SAR正侧视，首先目标P与雷达方位轨迹垂直距离为：$R_B=\sqrt{{y_p}^2+{z_p}^2}$，设法平面里雷达到 P 的侧视角为 β，即 $y_p=R_B\sin\beta$，$z_p=R_B\cos\beta$。那么辅天线瞬时斜距(式(3))转变为:

$$R_2=\sqrt{(x_{s1}-x_p+B\sin\alpha_{\mathrm{a}})^2+(B\cos(\alpha+\alpha_{\mathrm{r}})-R_B\sin\beta)^2+(B\sin(\alpha+\alpha_{\mathrm{r}})-R_B\cos\beta)^2}\approx R_B+\frac{(vt+\Delta x(t))^2}{2R_B}+\Delta R_{\mathrm{r}}(t) \quad (5)$$

其中 $x_{s1}-x_p=vt$，v 是 SAR 等效雷达速度，$\Delta x=B\sin\alpha_{\mathrm{a}}(t)$ 为水平抖动造成的方位向偏移，$\Delta R_{\mathrm{r}}=B\sin\beta\cos\ (\alpha+\alpha_{\mathrm{r}}(t))+B\cos\beta\sin(\alpha+\alpha_{\mathrm{r}}(t))$ 为基线抖动造成的瞬时斜距变化量。

方位多普勒信号的回波信号相位历程为 $-4\pi R_2/\lambda$，对公式(5)求方位时间 t 的 2 次导数，得到方位回波信号的瞬时调频率:

$$K_a=\frac{1}{2\pi}\frac{4\pi}{\lambda}\frac{\mathrm{d}^2R_2}{\mathrm{d}t^2}=\frac{2}{\lambda}\frac{\mathrm{d}^2R_2}{\mathrm{d}t^2}=\frac{2v^2}{\lambda R_B}+\frac{2(v\Delta x'+\Delta x'')}{\lambda R_B}+\frac{2\Delta R_{\mathrm{r}}''}{\lambda} \quad (6)$$

式中，$\Delta x'$，$\Delta x''$分别为Δx 对方位慢时间的一阶导数和二阶导数，$\Delta R_{\mathrm{r}}''$是ΔR_{r} 对方位慢时间的二阶导数。式(6)中第一项为不存在运动误差情况下方位向回波信号调频率，第二项是由于基线水平抖动造成的方位信号调频率的变化，此项随距离发生空变，由于分母上存在距离(R_B)项，所以相对第一项数值较小，可以忽略，也就是说基线水平抖动对于成像质量的影响是比较小的。式(6)中第三项调频率的误差为基线垂直抖动造成的，此项不可以忽略，使得方位向调频率产生误差，造成复图像方位向散焦。

3.2 基线抖动对干涉相位误差的影响

从辅天线复图像模型的角度，分析基线抖动带来的干涉相位误差模型。辅天线接收到的回波信号(式(4))经过距离压缩后，利用驻定相位原理，信号在距离多普勒域的表达式为:

$$s_{\mathrm{r}}(f_{\mathrm{a}},\tau)=A{w_{\mathrm{a}}}^2(f_{\mathrm{a}})\mathrm{sinc}\left[KT_{\mathrm{r}}(\tau-\frac{2R_{\mathrm{rd}}(f_{\mathrm{a}})}{\mathrm{c}})\right]\exp\left\{-\mathrm{j}\frac{4\pi}{\lambda}R_{\mathrm{rd}}(f_{\mathrm{a}})\right\} \quad (7)$$

式中 $R_{\mathrm{rd}}(f_{\mathrm{a}})$是多普勒域中的距离徙动，$R_{\mathrm{rd}}(f_{\mathrm{a}})=R_2(t_s)$，$t_{\mathrm{s}}$是驻定相位点。经过精确的距离徙动校正后，在频域内进行匹配滤波完成方位压缩，方位压缩后信号距离多普勒域变为:

$$s_1(f_{\mathrm{a}},\tau)=A{w_{\mathrm{a}}}^2(f_{\mathrm{a}})\mathrm{sinc}\left[KT_{\mathrm{r}}(\tau-\frac{2R_B}{\mathrm{c}})\right]\exp\left\{-\mathrm{j}\frac{4\pi}{\lambda}R_B\right\}\times\exp\left\{-\mathrm{j}\frac{4\pi}{\lambda}(\frac{\Delta x^2(t_{\mathrm{s}})+2vt_{\mathrm{s}}\Delta x(t_{\mathrm{s}})}{2R_B}+\Delta R_{\mathrm{r}}(t_{\mathrm{s}}))\right\} \quad (8)$$

式(8)即为最终复图像的距离多普勒谱，最后一个指数项为基线抖动带来的复图像多普勒谱相位误差项，经过方位向傅里叶逆变换后，这个指数项将产生额外的相位误差项，给最终的主辅天线干涉相位带来误差。对式(8)进行方位向傅里叶逆变换，得到点目标脉冲响应:

$$s_2(t,\tau)=A\mathrm{sinc}\left[KT_{\mathrm{r}}(\tau-\frac{2R_B}{\mathrm{c}})\right]\exp\left\{-\mathrm{j}\frac{4\pi}{\lambda}R_B\right\}\times\int_{-B_{\mathrm{d}}/2}^{B_{\mathrm{d}}/2}{w_{\mathrm{a}}}^2(f_{\mathrm{a}})\exp\left\{-\mathrm{j}\frac{4\pi}{\lambda}\Delta\phi(f_{\mathrm{a}})\right\}\exp(\mathrm{j}2\pi f_{\mathrm{a}}t)\mathrm{d}f_{\mathrm{a}} \quad (9)$$

式中 $\Delta\phi(f_{\mathrm{a}})=\frac{\Delta x^2(t_{\mathrm{s}})+2vt_{\mathrm{s}}\Delta x(t_{\mathrm{s}})}{2R_B}+\Delta R_{\mathrm{r}}(t_{\mathrm{s}})$ 为基线抖动造成的相位误差项。当不存在基线抖动时，此相位误差项为零，上式中的积分结果为 sinc 函数，即点目标脉冲响应与理想情况相一致。当此相位项不为零的时候，将对方位向成像进行调制，导致方位向散焦，这与前一节的分析是一致的，并且积分式会产生残留相位，导致辅天线相位产生误差，此相位误差即为基线抖动造成的干涉相位误差。由于方位向 $\frac{\Delta x^2(t_{\mathrm{s}})+2vt_{\mathrm{s}}\Delta x(t_{\mathrm{s}})}{2R_B}<<\Delta R_{\mathrm{r}}(t_{\mathrm{s}})$，可以予以忽略，利用驻定相位原理计算式(9)中的积分项，那么积分后相位项可以表示为:

$$\exp\left\{\mathrm{j}(-\frac{4\pi}{\lambda}\Delta\phi(f_{as})+2\pi f_{\mathrm{as}}t)\right\}=\exp\left\{\mathrm{j}(-\frac{4\pi}{\lambda}A_{\mathrm{r}}B\cos\beta\cos(\frac{2\pi f_{\mathrm{br}}}{K_{\mathrm{a}}}f_{as})+2\pi f_{\mathrm{as}}t)\right\} \quad (10)$$

式中，f_{as}为驻定相位点。式(10)即为基线抖动造成的干涉相位误差，由一个余弦函数和时间的线性函数组成。当 $2\pi(f_{\mathrm{br}}/K_{\mathrm{a}})f_{as}$ 接近 0 时，驻定相位点 f_{as} 和方位时间 t 是简单的线性关系，代入到干涉相位误差(式(10))中，得到干涉相位误差随方位时间变化表达式。根据相位误差公式，可以做出如下结论：①干涉相位误差近似满足正弦的变化关系；②相位误差变化频率正比于基线抖动频率。基线抖动频率越快，干涉相位误差变化也越快；③相位误差变化幅度正比于基线抖动幅度。基线抖动幅度越大，干涉相位误差变化幅度也越大，条纹越模糊。

4 仿真实例

为了验证上述基线抖动对成像质量和干涉相位影响的分析结果，根据建立的基线抖动瞬时斜距模型，将基线抖动影响引入到干涉 SAR 时域回波算法中生成回波信号，通过 SAR 成像得到干涉条纹。仿真采用 SRTM 任务中航天飞机轨道参数及其雷达参数，如表 1 和表 2。回波仿真模型包括：几何模型，后向散射模型和回波信号模型。几何模型考虑地球转动，地球椭球及曲线轨道的影响，如果在统一的惯性坐标系下计算，需要求解高次方程，为了简化计算，常采用空间直角坐标变换的方法(魏钟铨，2001)。电磁散射模型采用堪萨斯大学的 Ulaby 和密执安大学的 Dobson 建立了一种适合于更大入射角范围(入射角)的地面分布目标平均后向散射系数模型(Ulaby & Dobson, 1988):

$$\sigma^0(\mathrm{dB}) = P_1 + P_2\exp(-P_3\theta) + P_4\cos(P_5\theta + P_6) \quad (11)$$

式中，θ 是入射角(rad)，P_{1-6} 是由信号频率和地面分布目标类型共同确定的常数，一般是通过建立模型常数表查表得到的，回波算法采用距离时域脉冲相干法(刘永坦, 1999)。为了更好的说明基线抖动对成像质量的影响，首先进行点目标仿真，比较 SAR 成像的各项指标。然后针对人造场景进行面目标仿真，做成像处理后得到的干涉条纹图。

表 1 航天飞机轨道参数

轨道根数	数值
轨道周期/s	5349.0412
轨道近地点高度/km	220
轨道远地点高度/km	245
轨道高度/km	233
轨道倾角/(°)	57

表 2 雷达参数

雷达参数	数值
发射信号波长/m	0.03125
发射脉冲带宽/MHz	9.5
信号脉冲宽度/μs	40
脉冲重复频率/Hz	1488
数据采样率/MHz	11.4
波束中心视角/(°)	45
主天线尺寸/m^2	12×0.4
辅天线尺寸/m^2	12×0.4
有效基线长度/m	60

4.1 点目标仿真

为了验证基线抖动对成像质量的影响，采用点目标仿真说明。基线水平和垂直抖动幅度均为 0.025°，抖动频率 2Hz，生成点目标回波后进行脉冲压缩，压缩后得到点目标复图像方位向和距离向信号如图 2，图 2(a)中添加基线抖动前后距离向脉冲响应基本重合，说明基线抖动基本不对距离向成像产生影响。图 2(b)中方位向压缩信号相对理想压缩信号分辨率降低，峰值旁瓣比和积分旁瓣比相应增大，方位向出现散焦现象，且抖动频率和抖动幅度越大，方位向散焦越明显。

图 3 是验证基线水平抖动对成像质量的影响，基线水平抖动幅度 0.025°，抖动频率 4Hz，未添加基线垂直抖动。从图 3 可以看出，基线水平抖动添加前后，方位压缩信号基本上是重叠的，说明基线水平抖动对成像质量影响甚微。这跟第 2 节对于方位调频率误差第二项相较其他项数值较小可以忽略的分析是一致的。图 4 是点目标复图像多普勒谱相位差，实线是前面推导的理论计算值，见式(10)中的最后的相位项。可见理论值和点目标仿真值结果是相吻合的，成正弦关系变化。

4.2 面目标仿真

面目标仿真的目的是为了研究基线抖动对干涉相位图的影响。面目标仿真场景为(方位×距离) 512×2196 目标点，仿真地形数据为在场景中心人造锥形，

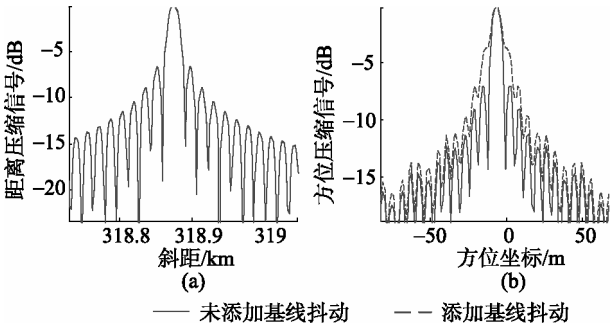

图 2 脉冲相应函数

(a) 距离压缩信号(实虚线基本重合); (b) 方位压缩信号

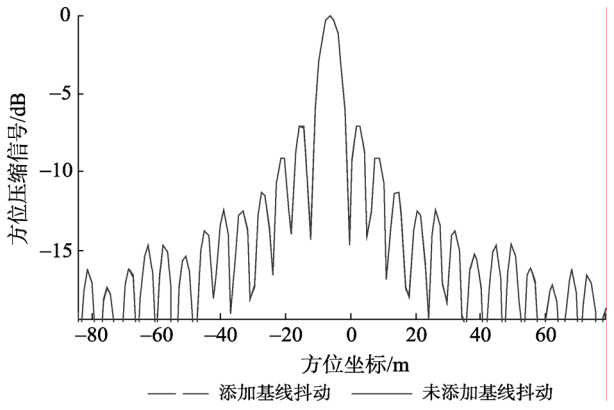

图 3 基线水平抖动对成像的影响(实虚线基本重合)

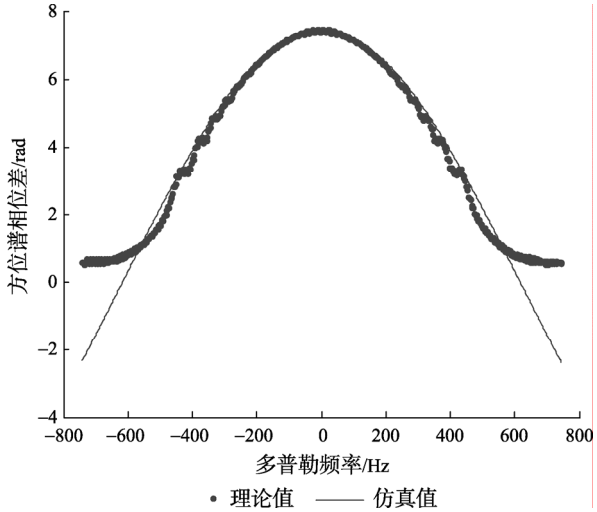

图 4 复图像方位谱比较

锥形峰值为 500 m。如图 5 所示，进行 SAR 回波信号计算和 SAR 成像，得到的干涉条纹随基线抖动程度的不同而变化的情况。由于干涉 SAR 条纹比较密集，为了较好的观看基线抖动对干涉相位的影响,将基线长度减为 4 m。干涉条纹发生了扭曲和模糊。图 5(a)是没有添加基线抖动误差的干涉条纹，条纹沿方位向未发生扭曲，条纹清晰可见(噪声点为回波信号中添加相干斑的缘故)。比较图 5(b)和图 5(c)发现当基线抖动幅度保持一致，基线抖动频率发生改变的时候，基线抖动频率越快，条纹发生扭曲的频率也越快，条纹的抖动的幅度相当。比较图 5(c)和图 5(d)可知，当抖动幅度增大的时候，相位误差的变化程度增大，条纹发生模糊。从图 5(d)中清晰可见在方位时刻，出现周期性的模糊，说明相位误差的周期性，这与本文讨论的是单频基线抖动，干涉相位误差也保持近似周期性的变化。这与第 2 节理论分析的结果是相吻合的。

图 6 给出了不同基线抖动幅度 A 和抖动频率 f 的情况下，干涉相位误差的比较情况(基线长度 60 m)。如图 6，当抖动幅度均为 0.05°，抖动频率分别为 2 Hz 和 4 Hz 时，相位误差近似正弦关系变化，且变化周期前者是后者的 2 倍，从图 6 看出，相位误差的变化周期跟基线抖动的周期是相等的；比较当抖动频率均为 2 Hz，抖动幅度分别为 0.05°和 0.1°时相位误差的变化，从图 6 看出，相位误差变化周期相同，但是基线抖动幅度越大，带来的干涉相位误差变化幅度也越大。这与 3.2 节理论分析的结果是相符的。

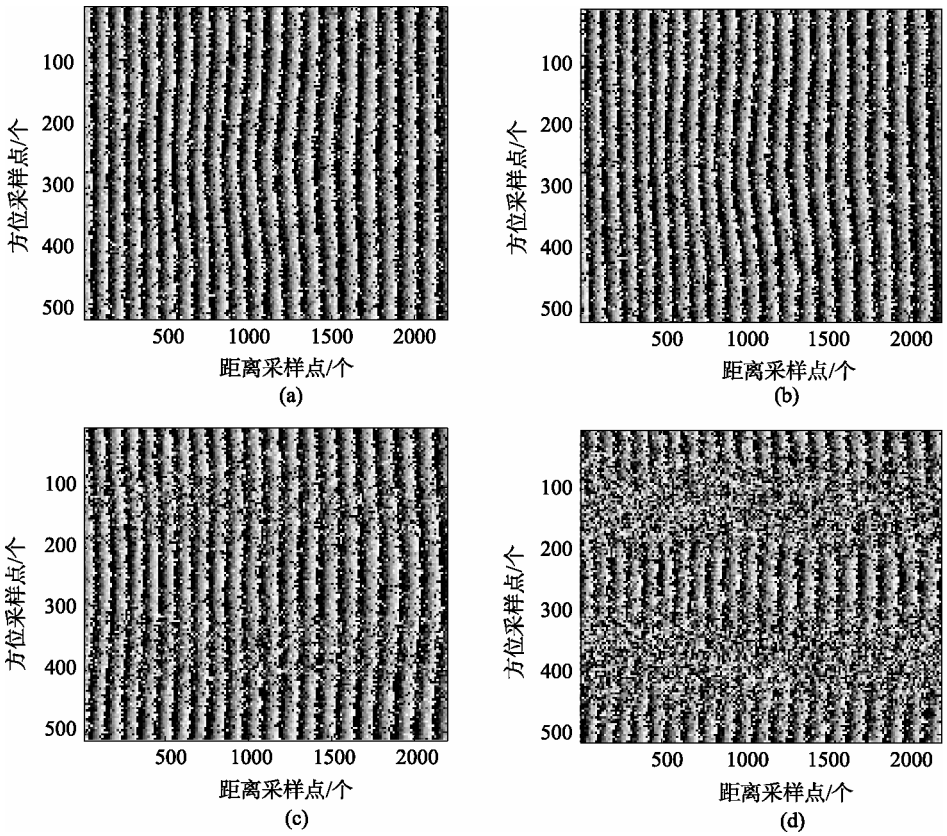

图 5 基线抖动对干涉条纹影响

(a) A=0, f=0; (b) A=0.05°, f=1Hz; (c) A=0.05°, f=3Hz; (d) A=0.1° , f=3Hz

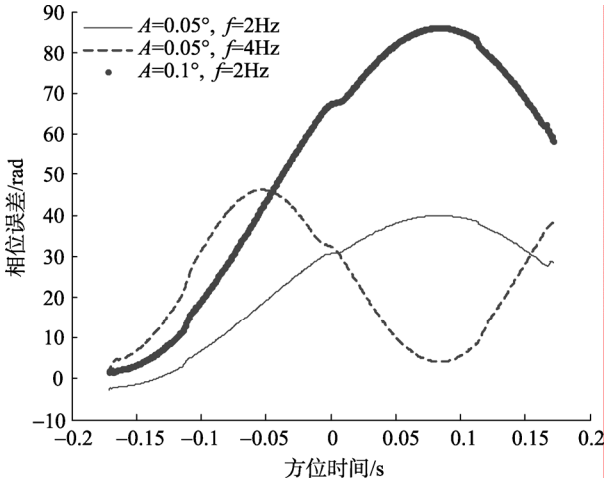

图 6　干涉相位误差

5　结　论

基于双天线干涉 SAR 基线抖动模型，建立了存在基线抖动情况下，辅天线复图像信号模型和干涉相位误差模型，分析了基线抖动对成像和干涉测量带来的影响，通过干涉 SAR 回波仿真，验证了理论分析的正确性。

REFERENCES

Bao Z, Xing M D and Wang T. 2005. Synthetic Aperture Radar Imaging. Beijing: Publishing House of Electronic Industry

Franceschetti G, Migliaccio M, Riccio D and Schirinzi G. 1992. SARAS: A synthetic aperture radar(SAR) raw signal simulator. *IEEE Trans. on Geoscience and Remote Sensing*, **30**(1): 110—123

Franceschetti G, Iodice A, Migliaccio M and Riccio D. 1998. A novel across-track SAR interferometry simulator. *IEEE Transactions on Geoscience and Remote Sensing*, **36**(3): 952—962

Franceschetti G, Iodice A, Maddaluno S and Ricco D. 2000. Effect of antenna mast motion on X-SAR/SRTM performance. *IEEE Trans. Geosci. Remote Sensing*, **38**(5): 2361—2372

Liu Y T.1999. Radar Imaging Technology. Haerbin: Harbin Institute of Technology Press

Mori A and Vita F D. 2004. A time-domain raw signal simulator for interferometric SAR. *IEEE Transactions on Geoscience and Remote Sensing*, **42**(9): 1811—1817

Ulaby F T and Dobson M C. 1988. Handbook of Radar Scattering Statistics for Terrain. Aretech House Editor

Wei Z Q. 2001. Synthetic Aperture Radar Satellite. Beijing: Science Press

附中文参考文献

保铮，邢孟道，王彤.2005.雷达成像技术. 北京：电子工业出版社

刘永坦. 1999. 雷达成像技术. 哈尔滨：哈尔滨工业大学出版社

魏钟铨. 2001. 合成孔径雷达卫星. 北京：科学出版社